# Supporting Information

# Vertical Macroporous Chitosan Aerogel Adsorbents for Simple and Efficient Enhancement of Atmospheric Water Harvesting and Air Dehumidification

Changhui Fu [a], Yuxuan He [a], Anhui Yu [a], Guangyi Tian [a], Danyan Zhan [a], Huimin Zhang [a], Zhiguang Guo [*a,b]

*a Ministry of Education Key Laboratory for the Green Preparation and Application of Functional Materials, Hubei University, Wuhan 430062, People's Republic of China.*

*b State Key Laboratory of Solid Lubrication, Lanzhou Institute of Chemical Physics, Chinese Academy of Sciences, Lanzhou 730000, People's Republic of China.*

***Corresponding Authors***

*Tel: 0086-931-4968105; Fax: 0086-931-8277088.*

*Email address: zguo@licp.cas.cn (Z Guo).*

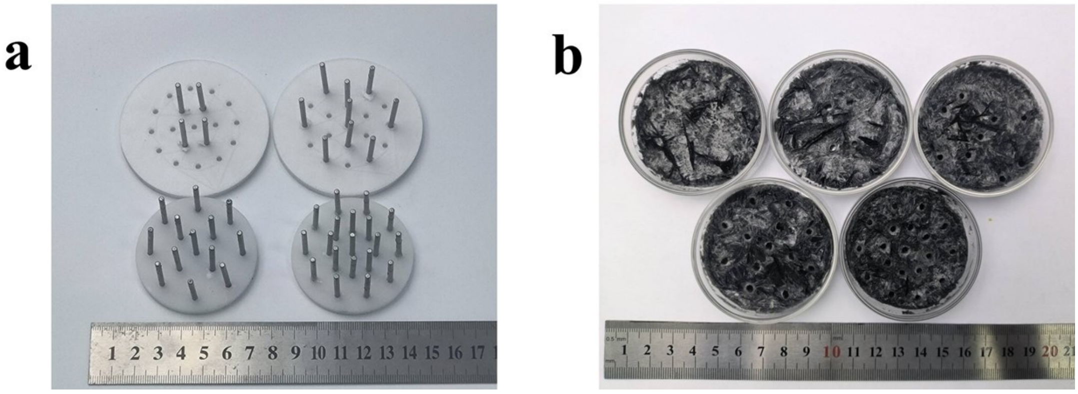


Figure S1. (a) Optical photographs of cylindrical steel needle templates with different numbers of needles. (b) Optical photographs of CSC-MC with different numbers of macroporous channels

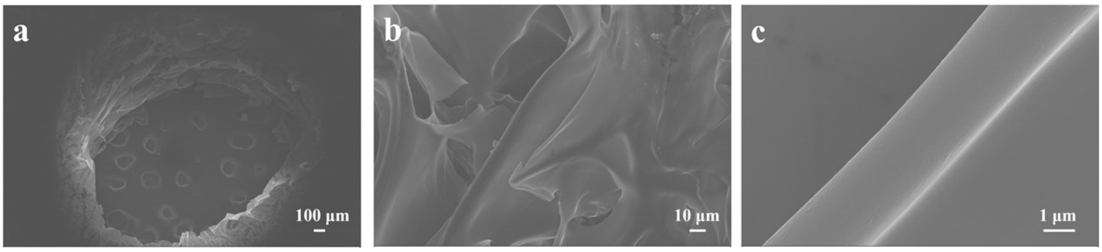


Figure S2. (a-c) SEM images and further magnified SEM images of CS-MC aerogel with smooth surface.

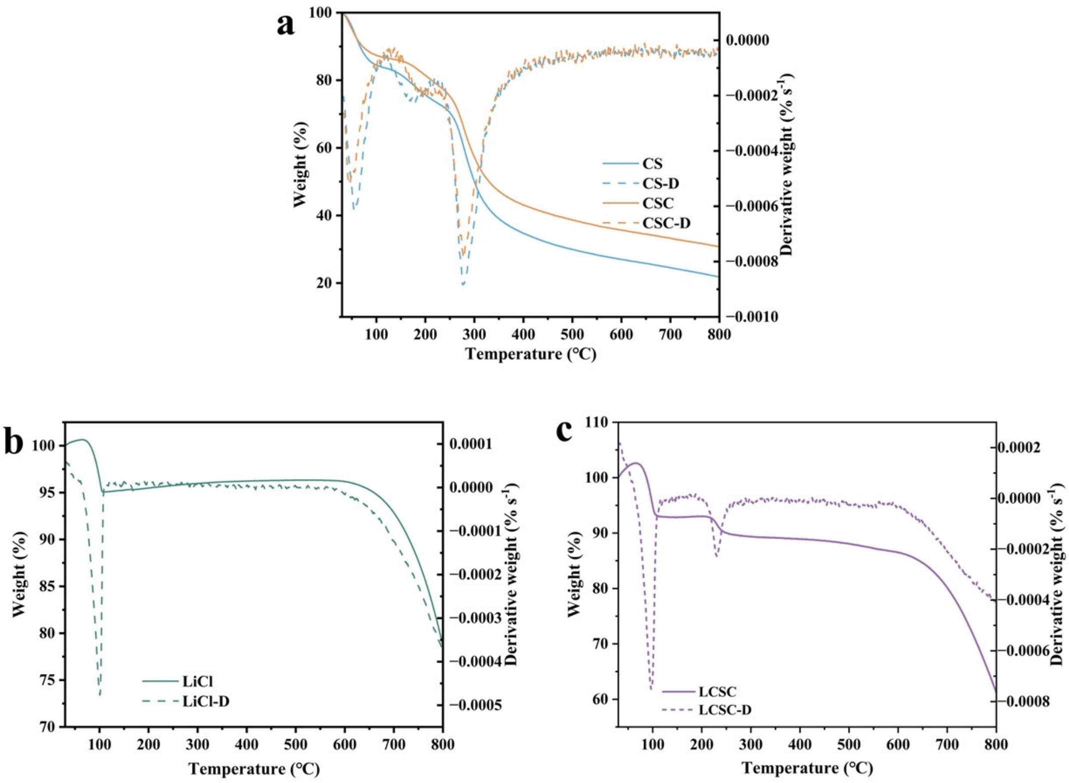


Figure S3. (a) TGA results of CS and CSC aerogels and corresponding DTG curves. (b) TGA results of LiCl and corresponding DTG curves. (c) TGA results of LCSC aerogel and corresponding DTG curves.

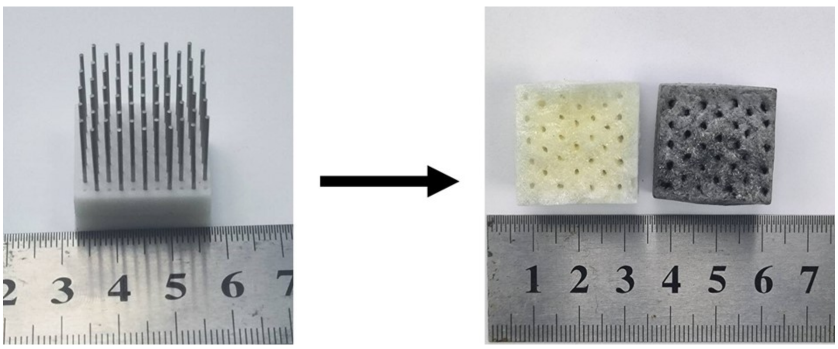

Figure S4. Small-size needle array template (cylindrical needles with a diameter of 0.8 mm) and a diagram of a sample prepared using the small-size template.

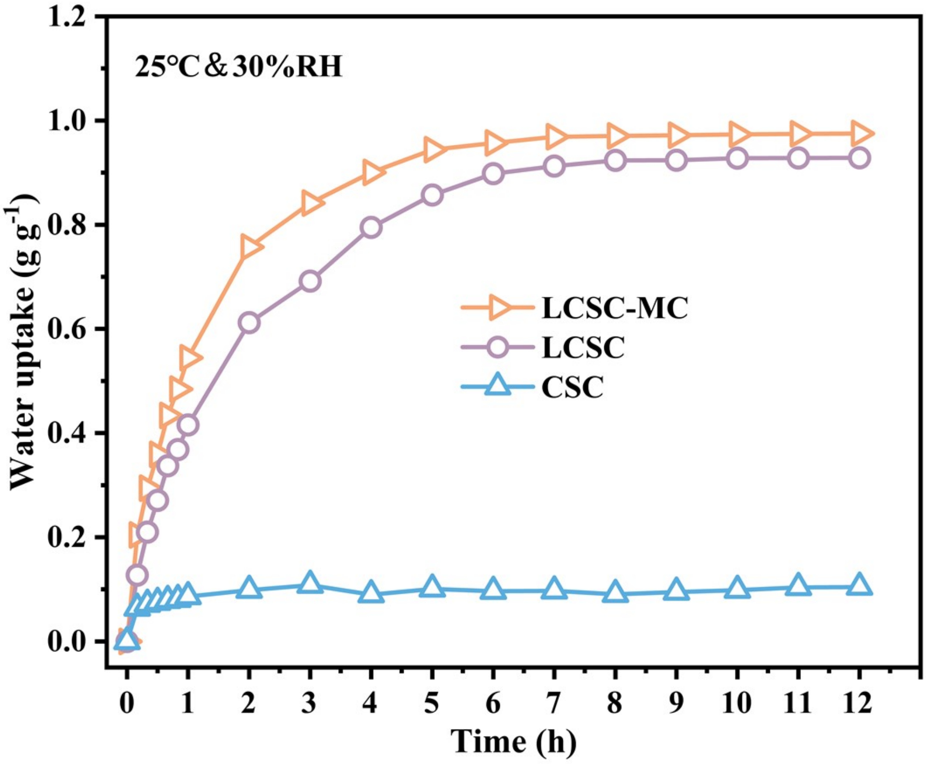


Figure S5. Dynamic water vapour adsorption process of small size scale aerogel adsorbents at 30% RH and 25 °C.

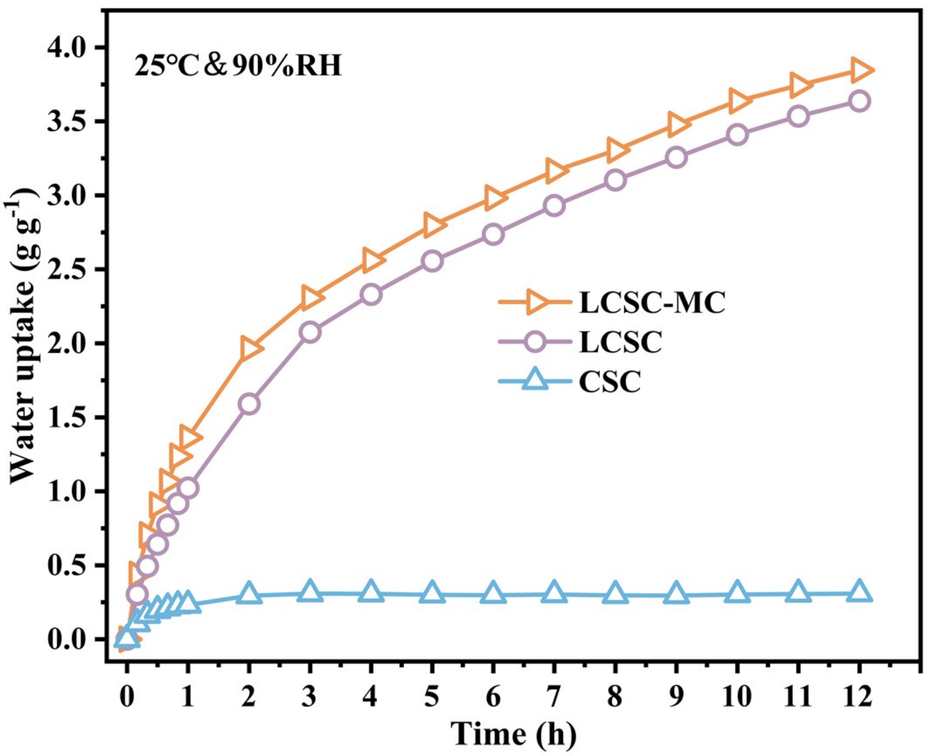


Figure S6. Dynamic water vapour adsorption process of small size scale aerogel adsorbents at 90% RH and 25 °C.

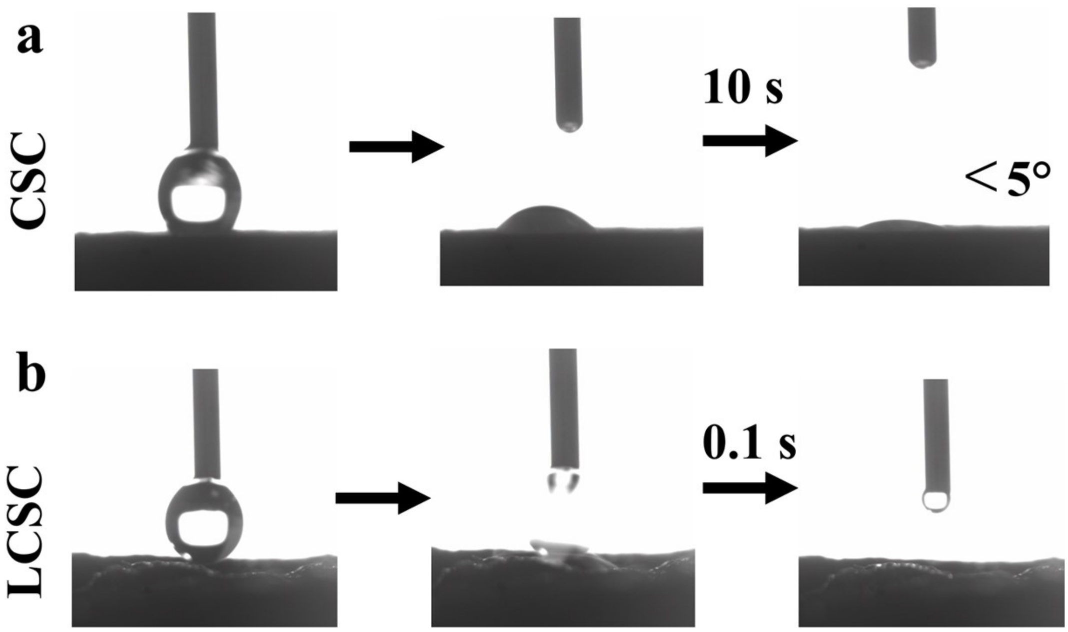


Figure S7. (a) Change in water contact angle (WCA) of water droplets on the CSC aerogel surface. (b) WCA of water droplets on the LCSC aerogel surface and instantaneous wetting phenomenon.

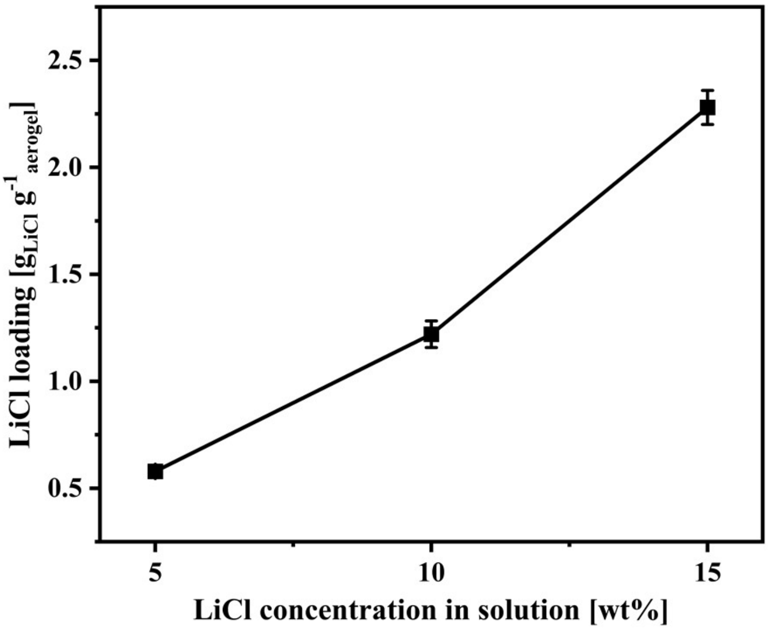


Figure S8. The amount of salt loading for immersion in different concentrations of lithium chloride.

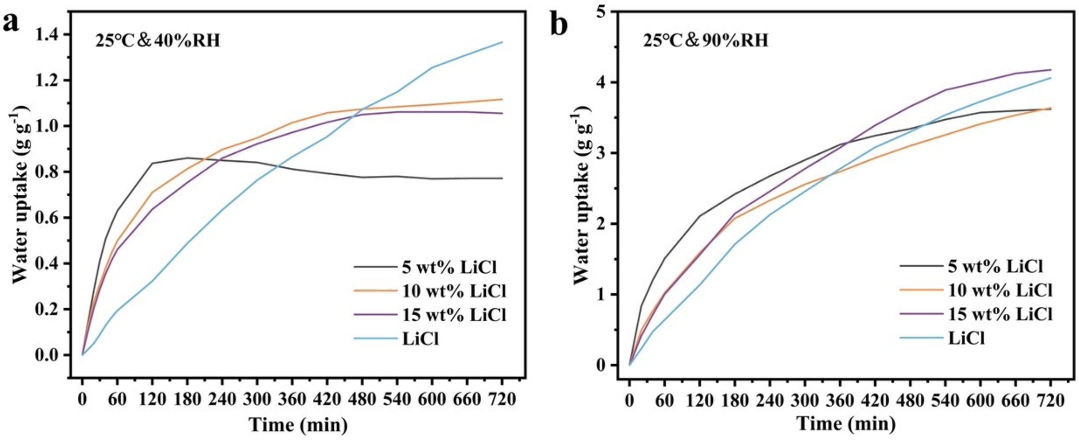


Figure S9. (a) Water absorption of LCSC aerogels with different LiCl loadings and lithium chloride at 40% relative humidity. (b) Water absorption of LCSC aerogels with different LiCl loadings and lithium chloride at 90% relative humidity.

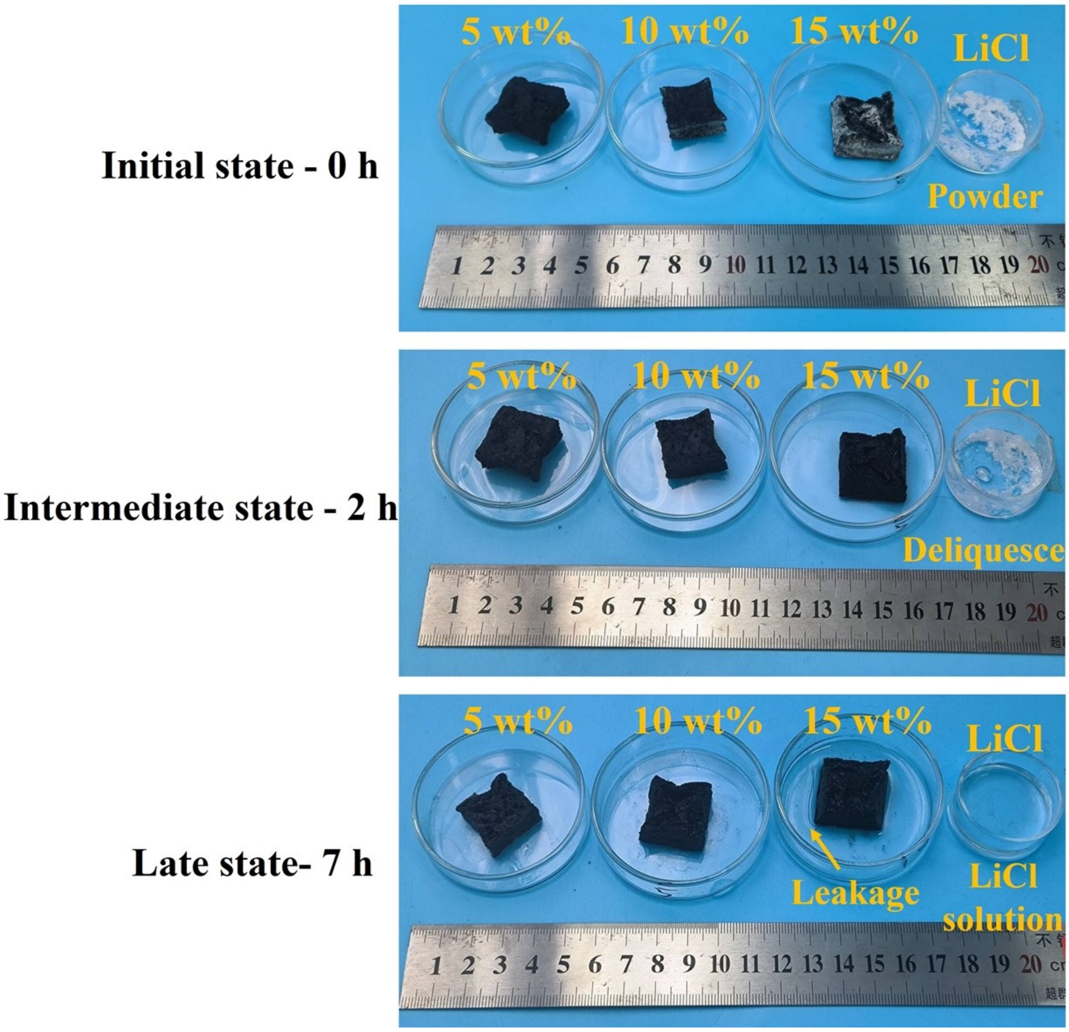


Figure S10. Optical photographs of LCSC aerogels with different lithium chloride loadings and pure lithium chloride in different hygroscopic phases at 90% RH.

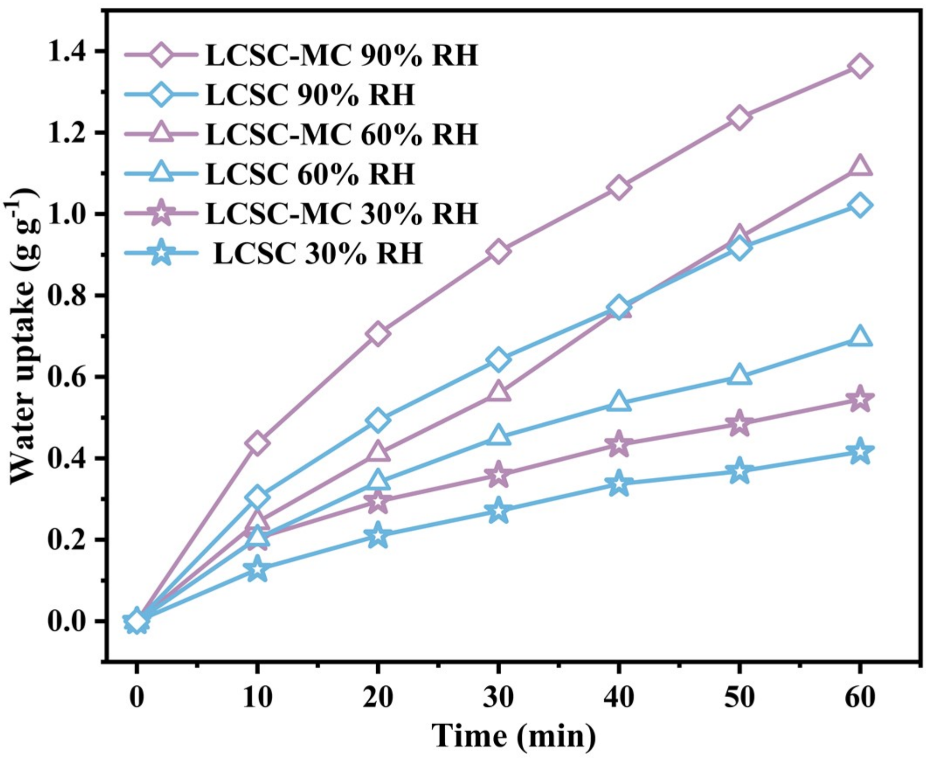


Figure S11. Dynamic hygroscopicity curves of small size scale LCSC-MC and LCSC aerogel adsorbents at different humidity for 1 hour.

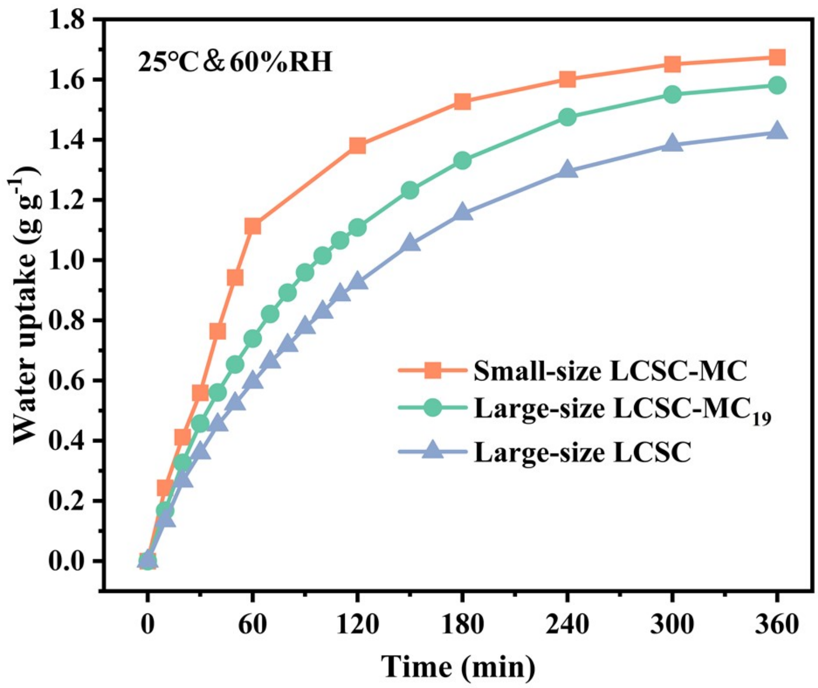


Figure S12. Comparison of water absorption between small size sample and large size samples.

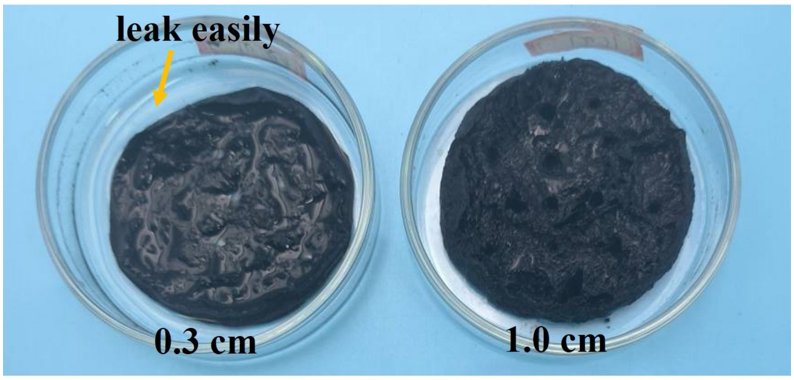


Figure S13. Optical photographs of LCSC-MC of 0.3 cm and 1 cm thickness after moisture absorption at 80% RH for 5 hours.

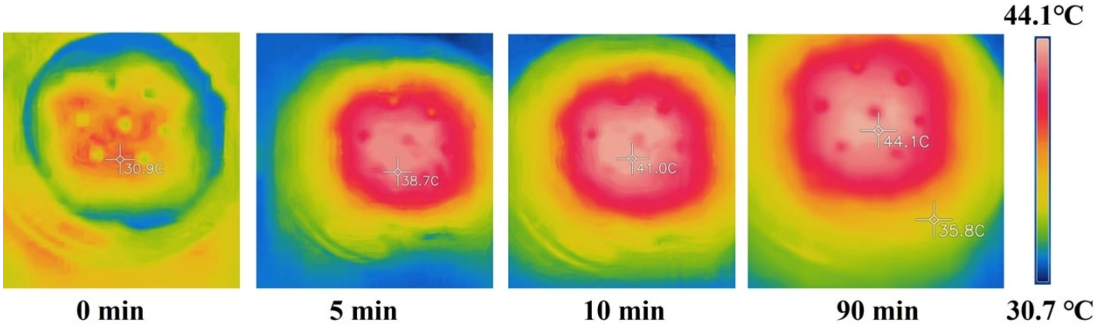


Figure S14. Infrared thermal images of the surface of LCS-MC aerogel after moisture absorption at 1000 W/m$^2$ light intensity and the final temperature field within 1.5 h of irradiation.

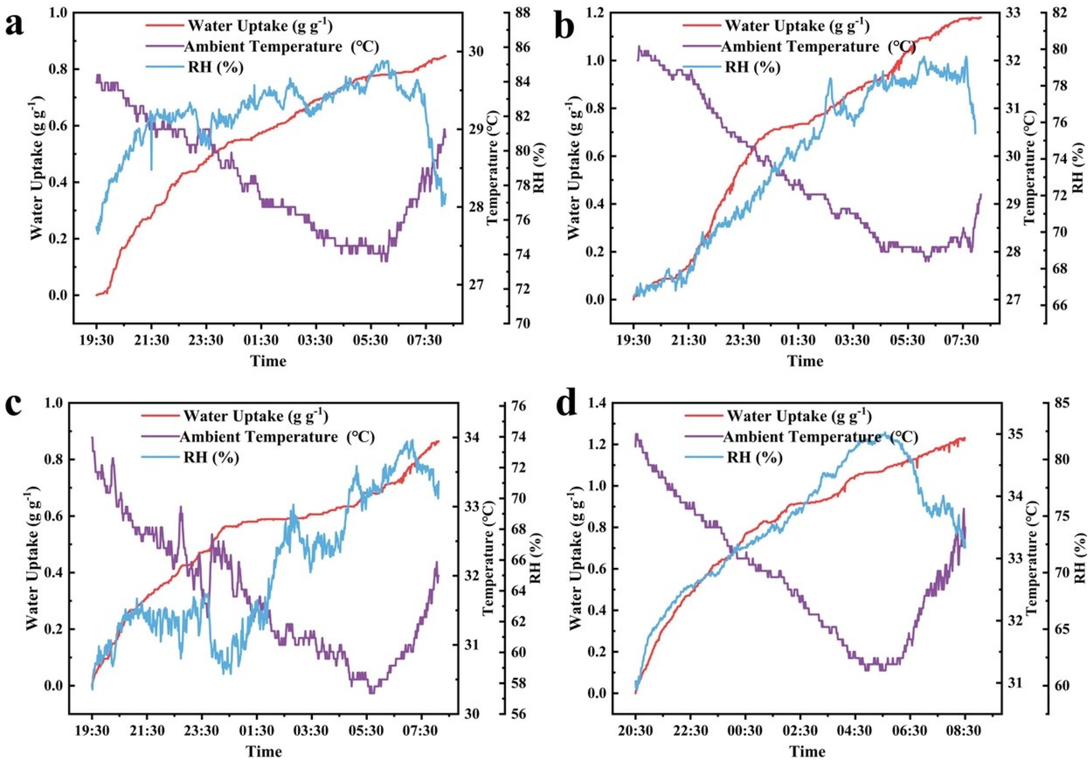


Figure S15. Multiple water absorption tests under outdoor environment.

Table S1. Comparison of hygroscopic properties of materials used for AWH reported in other literatures.

| AWH materials | RH (%) | Water uptake (g/g) | References |
|---|---|---|---|
| PPy-COF@Trilayer-LiCl | 30 | 0.77 | [1] |
| | 60 | 1.37 | |
| Pollen-LiCl@PNIPAM-b-Ppy | 20 | 0.4 | [2] |
| | 60 | 1.1 | |
| | 80 | 1.58 | |
| MAWH | 90 | 3.12 | [3] |
| MOF-801 | 30 | 0.19 | [4] |
| | 50 | 0.23 | |
| | 60 | 0.25 | |
| | 90 | 0.29 | |
| CAL gel | 20 | 0.63 | [5] |
| | 30 | 0.79 | |
| | 70 | 1.65 | |
| FES500@Li aerogel | 30 | 0.48 | [6] |
| | 60 | 1.15 | |
| | 90 | 3.29 | |
| CA@STH-MPN | 30 | 0.66 | [7] |
| | 40 | 0.9 | |
| | 60 | 1.35 | |
| | 80 | 1.91 | |
| | 90 | 2.29 | |
| LCSC-MC | 20 | 0.75 | This work |
| | 40 | 1.11 | |
| | 60 | 1.71 | |
| | 80 | 2.55 | |
| | 90 | 3.85 | |

Table S2. Specification and cost of materials used in the experiment

| Raw materials | Specification | Price ($) |
|---|---|---|
| Chitosan | 500 g | 43.25 |
| Nanocarbon | 25 g | 21.68 |
| LiCl | 500 g | 17.97 |
| LCSC-MC | 1.25 g CS, 0.15 g nanocarbon, 10 g LiCl | 0.6 |

Supplementary note: A single experiment to prepare LCSC-MC with 50 g of total precursor solution required 1.25 g of CS, 0.15 g of nanocarbon powder, and 100 g of an aqueous solution of LiCl with 10 g of LiCl solids. Thus a sample prepared in 50 ml of total solution precursor costs only $ 0.6. It should be noted that when raw materials are purchased on a large scale, this will further reduce costs.


[1] M. Xia, D. Cai, J. Feng, P. Zhao, J. Li, R. Lv, G. Li, L. Yan, W. Huang, Y. Li, Z. Sui, M. Li, H. Wu, Y. Shen, J. Xiao, D. Wang, Q. Chen, *Advanced Functional Materials* **2023**, 33, 2214813.

[2] X. Zheng, Q. Ma, T. Wan, W. Wang, Q. Pan, R. Wang, *Advanced Functional Materials* **2024**, n/a, 2407127.

[3] C. Cai, Y. Chen, F. Cheng, Z. Wei, W. Zhou, Y. Fu, *ACS Nano* **2024**, 18, 4376.

[4] C. Yang, H. Wu, J. Yun, J. Jin, H. Meng, J. Caro, J. Mi, *Advanced Materials* **2023**, 35, 2210235.

[5] H. Zhou, L. Yan, D. Tang, T. Xu, L. Dai, C. Li, W. Chen, C. Si, *Advanced Materials* **2024**, 36, 2403876.

[6] N. Ding, B. Liang, X. Gao, D. Yao, J. Chen, C. Liu, C. Lu, X. Pang, *Chemical Engineering Journal* **2024**, 495, 153470.

[7] Y. Bu, X. Li, W. Lei, H. Su, H. Yang, W. Xu, J. Li, *Journal of Materials Chemistry A* **2023**, 11, 15147.